Stratified Layer Flow Model: A Numerical Approach to Liquid Temperature Stratification

G. C. VLIET,* J. J. BROGAN,† T. S. SHEPPARD,‡ F. H. MORSE,§ AND F. L. HINES¶
Lockheed Missiles and Space Company, Sunnyvale, Calif.

A physical model for temperature stratification in liquids contained in heated nondraining vessels is presented. The model recognizes the natural convection boundary layer, which develops along the heated walls of the vessel and transports warm fluid to the surface as being the primary mechanism of stratification. Interaction between the boundary-layer flow and previously stratified fluid in the model is determined from energy and mass balance considerations. The liquid and its vapor are thermodynamically coupled by allowing mass and energy transfer at the vapor-liquid interface. The flow model and its governing equations as programed on a digital computer are described. Numerical results obtained from the flow model are shown to compare well with experimental data.

Nomenclature

A_B = area below start of boundary layer
c_L = liquid specific heat
g = acceleration
g_0 = one standard gravity
g^* = number of standard gravities
i = index used to denote time step
k = thermal conductivity
K = index denoting layer number
M_u = ullage mass
ΔM = mass vaporized
P_u = ullage pressure
q_u = ullage heat rate
q_L = bottom heat leak
q_w'' = wall heat flux
R = tank radius
R_a^* = modified Rayleigh number
T_B = unstratified liquid temperature
T_{BL} = mixed mean boundary-layer temperature
T_L = local bulk temperature
T_u = ullage temperature
T_w = wall temperature
$\bar{T}(\ )$ = indexed average layer temperature
u = velocity
u^* = fictitious boundary-layer velocity
$u_{\max}$ = maximum boundary-layer velocity
$\bar{u}$ = average boundary-layer velocity
$W(\ )$ = indexed layer mass
W_B = mass of unstratified liquid
W_T = total liquid mass
x = boundary-layer coordinate
$\Delta x(\ )$ = indexed layer thickness
y = distance normal to wall
z = axial coordinate
β = volumetric coefficient of thermal expansion
δ = boundary-layer thickness
$\Delta z(\ )$ = indexed layer thickness
$\Delta\theta$ = time step
μ = viscosity
ν = kinematic viscosity
ρ = density
ϕ = half-angle of vessel bottom

Subscripts

f = final condition
i = initial condition
s = surface condition
1 = condition at layer top
2 = condition at layer bottom

Presented as Preprint 64-37 at the AIAA Aerospace Sciences Meeting, New York, January 20–22, 1964; revision received June 24, 1964. This work was conducted under Contract NAS 8-5600.

* Associate Research Scientist.
† Head, Cryogenics Analysis, Large Space Vehicle Programs.
‡ Research Specialist; now at Grumman Aircraft Co., Beth Page, N. Y.
§ Scientist.
¶ Research Specialist. Member AIAA.

Introduction

THE need for accurate prediction and understanding of temperature stratification in fluids contained in heated vessels has increased recently because of the influence of this phenomenon on the design of space vehicles. As a result of the relatively low temperature of a cryogenic liquid, heat is transferred by conduction through the insulated walls of the vessel and the heated liquid near the walls flows toward the liquid surface under the action of buoyant forces. This continuous convection process results in a temperature variation (temperature stratification) in the liquid below the surface, the temperature and depth of the stratified region increasing with time. Temperature stratification is important in the design of propellant tanks because the tank design pressure increases with the severity of the temperature variation within the liquid.** For example, in the case of liquid hydrogen, each 1°R rise in the liquid vapor interface temperature represents approximately a 3 psia rise in ullage pressure. For a large space vehicle each psia rise in design pressure increases the tank weight several hundred pounds. Therefore, an adequate means of predicting temperature stratification is essential.

Probably the first attention brought to temperature stratification was the experimental data obtained by Huntley[1] and Scott et al.[2] In the past year a considerably greater interest in this subject has been shown by the amount of work being done in this field. Bailey et al.[3] and Bailey and Fearn[4] present some data and a simplified analysis for stratification of liquid hydrogen. Tatom et al.[5] present experimental data for stratification in liquid hydrogen and an analysis that uses empirical constants obtained from the data. Tellep and Harper[6] present experimental data for water which are compared to their approximate integral analysis. The analysis assumes the dimensionless temperature profiles on the stratified region are time invariant, bases the stratified layer growth rate on the boundary-layer flow at the base of the region, and accounts for phase change at the vapor-liquid interface.

** In practice there would be a tradeoff between increasing tank weight and vaporizing a portion of the warm liquid near the surface.

Table 1 Natural convection flow and stratification regimes

Ra^*	Nature of flow	Nature of stratification
<1	Conduction governs energy transfer	Liquid temperature varies axially and radially
1 to 10^5	Viscous flow throughout	
10^5 to 10^{11}	Laminar boundary layer	Axial variation of temperature in stratified region
$>10^{11}$	Turbulent boundary layer	

Flow visualization studies of stratification have been made in water by Schwind and Vliet[7] using the schlieren technique and the dye trace method. These studies indicate some of the more detailed aspects of stratification, namely, the nature of the boundary-layer flow as affected by the presence of positive temperature gradients and the nature of the surface flow. Anderson and Kolar[8] have performed studies that include both wall and volume heating. Both schlieren studies and temperature measurements were performed. Analyses of turbulent natural convection boundary-layer flow have been performed by Eckert and Jackson,[9] Bayley,[10] and Fujii.[11]

Temperature stratification in liquids can arise from various sources, including 1) natural convection of warm liquid along the heated container walls toward the surface, 2) convection resulting from nuclear energy absorption in the propellant of a nuclear powered rocket, and 3) energy and mass transfer between the liquid and the ullage. The importance of each source depends on the relative effort made in insulating the vessel against thermal and nuclear energy and upon the pressurant used and its temperature. In general, wall heating contributes most to the formation of the stratified region. Nuclear energy absorption has the effect of producing a region of uniform temperature, and the effect of phase change at interface is confined mainly to only a thin region of liquid near the surface.

The nature of the stratification due to wall heating is strongly influenced by the gravitational as well as the thermal environment. The magnitude of the modified Rayleigh number

$$Ra^* = \left(\frac{g\beta q_w'' x^4}{k\nu^2}\right)\left(\frac{c_L \mu}{k}\right)$$

indicates the character of the natural convection flow and also the resulting nature of the stratification. Table 1 indicates both the type of flow and resulting temperature distribution as functions of the modified Rayleigh number for an axisymmetric vessel. For Ra^* less than approximately 10^5, the resulting fluid temperature will vary both axially and radially, since either conduction will dominate energy transfer or the fluid is in gross viscous flow throughout. For Ra^* greater than approximately 10^5 the boundary layer is thin compared to the dimensions of the vessel. At these large values of Ra^*, the Rayleigh number based on stratified layer depth

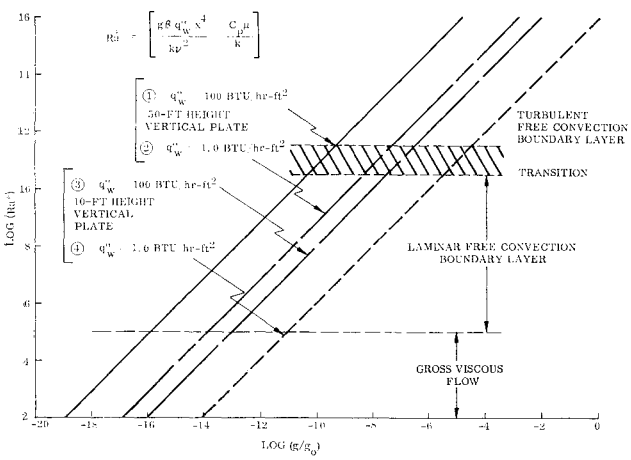

Fig. 1 Flow regimes for liquid hydrogen.

(which indicates the thermal stability of the fluid) will most certainly insure that, except for the thin boundary layer, the isotherms in the fluid are essentially horizontal. The thermal gradients in the stratified fluid are, therefore, parallel to the acceleration vector and a simplified one dimensional approach to stratification should be a good representation in the region $Ra^* > 10^5$.

Figure 1 represents the boundary-layer flow regimes for liquid hydrogen (equivalent curves for liquid oxygen would be shifted to the right about 1 decade), for typical characteristic lengths and heat fluxes. A comparison of Fig. 1 with the magnitudes of acceleration listed in Table 2 indicates that one-dimensional stratification will exist for almost all space missions. The first four sources of thrust definitely fall in the turbulent natural convection boundary-layer regime of Fig. 1. One source of acceleration that is always present is radiation pressure, which falls in the laminar free convection boundary-layer regime of Fig. 1.

This paper presents a numerical approach, called the stratified layer flow model, to the problem of temperature stratification in liquids contained in heated vessels. Results of applying this model using an IBM 7090 computer are presented and discussed. The model as programed for computer solution uses turbulent boundary-layer equations and, therefore, is applicable only in the case where $Ra^* > 10^{11}$. However, the model could easily be programed for laminar natural convection boundary-layer flow and used for $10^5 < Ra^* < 10^{11}$. A complete description of the model is available in Ref. 12.

The Stratified Layer Flow Model and Analysis

The growth of the stratified region results from the continuous supply of liquid at its base and the temperature variation within the region is determined by the continuous interaction of the region with the boundary-layer flow through it, the conduction within the layer itself and the interaction between the layer and the vapor above it at the surface. The model developed to represent this continuous process uses a time-step approach. At any particular instant of time, the stratified region is composed of several layers (Fig. 2). The natural convection boundary layer, which is assumed to be in steady state during each time step, is based on the heat flux and acceleration at the midpoint of the time step and on the bulk liquid temperature distribution at the beginning of the step. For each time step a new layer is formed at the surface due to the natural convection boundary-layer flow that reaches the surface†† during the time step. Any liquid

Table 2 Accelerations on space vehicles

Source	Acceleration, g^*
Earth gravity, prelaunch	1
Typical space vehicle thrusts	0.1 to 10
Atmospheric drag, low earth orbit	10^{-4}
Venting thrust	10^{-4}
Centripetal, preferred vehicle orientation: low earth orbit	10^{-6}
Centripetal, preferred vehicle orientation: interplanetary	10^{-14}
Radiation pressure (near earth)	10^{-10}

†† The boundary layer initiates at a specified point in the vessel bottom and is assumed to be unaffected by the vapor-liquid interface, although distortion will occur in the vicinity of the interface.

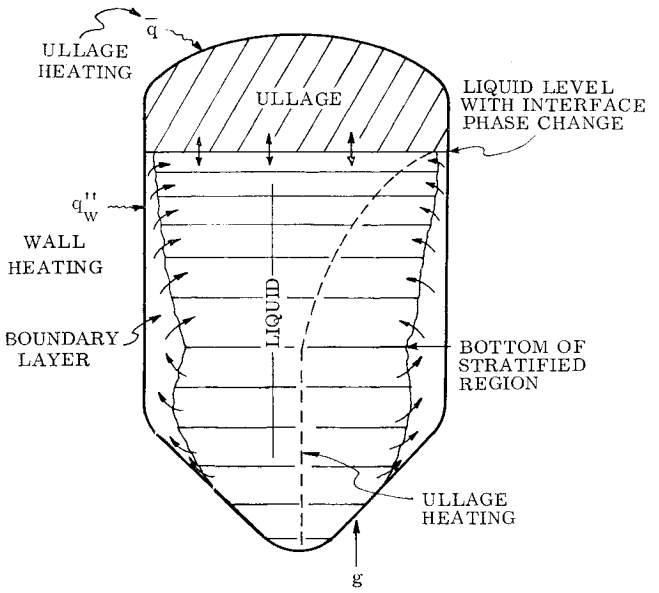

Fig. 2 Physical flow model.

entrained by or rejected from the boundary layer as it flows through each previously stratified layer is, respectively, deleted from or uniformly mixed with the liquid of that layer. The energy entering the vessel below the point of boundary-layer initiation is then mixed into the unstratified bulk liquid. The new top layer is then allowed to interact with the ullage region, that is, interface mass and energy transfer are permitted so that the ullage pressure and surface liquid vapor pressure equalize. The program then proceeds to the next step.

The program uses a liquid and its vapor in equilibrium (saturated state) as the initial condition. The inputs include 1) tank geometry (an axisymmetric vessel such as shown in Fig. 2), 2) side wall heat input to the liquid region (uniform over the entire surface area and time dependent), 3) a time dependent acceleration environment, 4) location of initiation of boundary layer in vessel bottom, 5) ullage heat input and ullage volume, 6) size and number of time steps, 7) the total mass of liquid, and 8) necessary physical constants (fluid properties, etc.).

The First Time Step

Initially, the temperature is uniform throughout liquid and vapor, and stratification begins when the vessel is closed. Thus the natural convection boundary-layer equations for the first time step are integrated from the tank bottom to the liquid surface based on a uniform bulk temperature and the heat flux and acceleration at the middle of the time interval. The boundary-layer equations are described in detail in a later section. The total boundary-layer flow, reaching the surface over the time step, is deposited in a layer (disk) of uniform thickness below the surface and exterior to the boundary layer as shown in Fig. 3. The mass deposited in the layer and the layer thickness are

$$W(1) = 2\pi\rho R_s\delta_s\bar{u}_s\Delta\theta \tag{1}$$

$$\Delta z(1) = W(1)/\pi\rho(R_s - \delta_s)^2 \tag{2}$$

The average temperature of the layer is the mixed mean boundary-layer temperature at the surface

$$\bar{T}(1) = T_{L,s} + C_1 q_w''\delta_s^{1/4}/\bar{u}_s^{3/4} \tag{3}$$

where $T_{L,s}$ is the local bulk temperature at the surface, and C_1 is a constant including fluid properties. Following the deposition of the first layer, all the energy entering the vessel below the point of boundary-layer initiation is assumed to uniformly mix into the unstratified mass. This energy $(q_w''A_B + q_L)\Delta\theta$, mixes into the unstratified mass $W_T - W(1)$ increasing its temperature by

$$\Delta T_B = (q_w''A_B + q_L)\Delta\theta/c_L[W_T - W(1)] \tag{4}$$

and the bulk temperature is adjusted accordingly.

To conserve energy and to eliminate a temperature discontinuity at the bottom of this first layer, a linear temperature gradient through the layer is assumed. Thus, the temperature at the bottom of the layer is set equal to the bulk temperature T_B, and the temperature at the center of the layer is set to $\bar{T}(1)$, the average boundary-layer temperature at the surface. The top layer is then allowed to interact with the ullage to establish equilibrium between the ullage pressure and the surface liquid vapor pressure, as described subsequently. The result of the mass and energy transfer due to phase change is that the top layer has a new mean final temperature and mass, and the ullage has a new mass, pressure, and average temperature. The program then proceeds to the second time step.

The ith Time Step

At the end of the $(i\text{-}1)$ time step, $(i\text{-}1)$ layers have been formed. The mean temperature, mass, thickness, and position of each layer are specified. The temperature profile through the stratified region is obtained by connecting the mean temperatures (located at the layer centers) of adjacent layers. The bottom of layer 1 is at the uniform bulk temperature and the line connecting $\bar{T}(i\text{-}2)$ and $\bar{T}(i\text{-}1)$ is extended to the liquid surface. The ullage region has a prescribed mass, temperature, and pressure.

The boundary-layer equations are integrated from the tank bottom to the liquid surface through the stratified layers, using the bulk temperature distribution at the end of the $i\text{-}1$ step and the values for heat flux and acceleration at the middle of the ith step. It is found that the boundary-layer

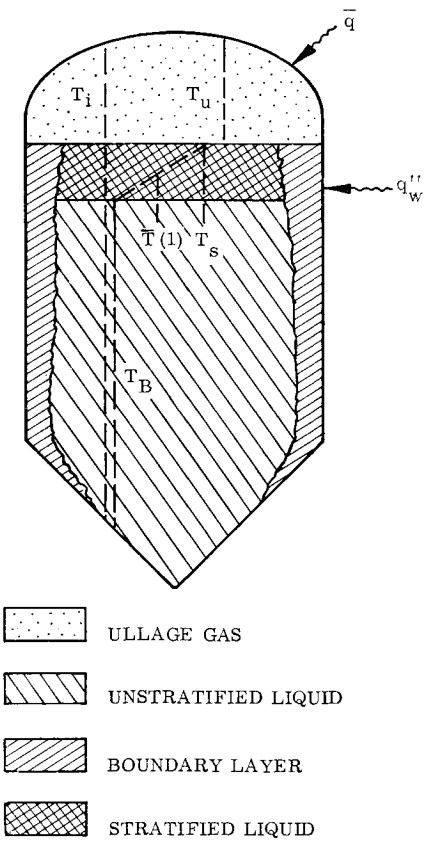

Fig. 3 The first time step.

thickness will either increase or decrease depending primarily on the bulk temperature gradient, and therefore, the boundary-layer flow through the stratified region can cause layers to either increase or decrease in mass. Mass and energy balances are performed on each of the i-1 layers as depicted in Fig. 4 for layer K. The new mass $W_n(K)$ of layer K is

$$W_n(K) = W(K) + 2\pi\rho(R_2\bar{u}_2\delta_2 - R_1\bar{u}_1\delta_1)\Delta\theta \quad (5)$$

where δ_1 and $\bar{u}_1$ are the boundary-layer thickness and average velocity at the top of layer K, and δ_2 and $\bar{u}_2$ are the corresponding values at the bottom of the layer. The boundary layer mixed mean temperature at the top of layer K is

$$T_{BL,1} = T_{L,1} + C_1 q_w''\delta_1^{1/4}/\bar{u}_1^{3/4} \quad (6)$$

and $T_{BL,2}$, the boundary-layer mixed mean temperature at the bottom, is calculated in a similar fashion, where $T_{L,1}$ and $T_{L,2}$ are the local bulk liquid temperatures at the top and bottom of layer K, respectively. The new average temperature of layer K is, therefore,

$$\bar{T}_n(K) = \{W(K)\bar{T}(K) + 2\pi\rho[R_2\bar{u}_2\delta_2 T_{BL,2} - R_1\bar{u}_1\delta_1 T_{BL,1}]\Delta\theta + \pi[(R_1 + R_2)\Delta x(K)q_w''/c_L]\Delta\theta\}/W_n(K) \quad (7)$$

A new top layer (the ith layer) is formed as a result of the accumulated boundary-layer flow at the liquid surface, which, over the time step $\Delta\theta$, is

$$W(i) = 2\pi\rho R_s\delta_s\bar{u}_s\Delta\theta \quad (8)$$

and the average temperature at which it is deposited (i.e., the mixed mean temperature of the boundary layer at the surface) is

$$\bar{T}(i) = T_{L,s} + C_1 q_w''\delta_s^{1/4}/\bar{u}_s^{3/4} \quad (9)$$

Following the deposition of the new top layer all energy entering the vessel below the point of boundary layer initiation is uniformly mixed into the unstratified mass in the same manner as for the first time step except that the unstratified mass W_B is now

$$W_B = W_T - \sum_{K=1}^{i} W(K) \quad (10)$$

The top layer is then permitted to interact with the ullage (similar to that described for the first time step) to give a new mass and temperature of the top layer and new mass, pressure, and average temperature of the ullage.

Negative vertical temperature gradients between layers may result from abnormally high vaporization of the top layer or possibly may be due to sharp changes in boundary-layer flow between layers. The model assumes that negative vertical temperature gradients between layers cannot exist because turbulent mixing would result from the unstable density inversion. The program employs a mixing routine that compares the temperatures of all adjacent layers and successively mixes any adjacent layers possessing negative temperature gradients until only positive or zero temperature gradients between layers exist. The layers are assumed to retain their initial masses but their temperatures are equalized under the constraint of energy conservation.

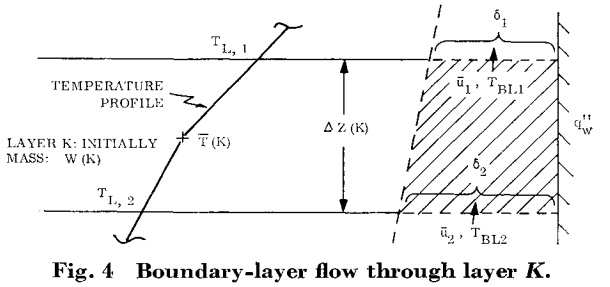

Fig. 4 Boundary-layer flow through layer K.

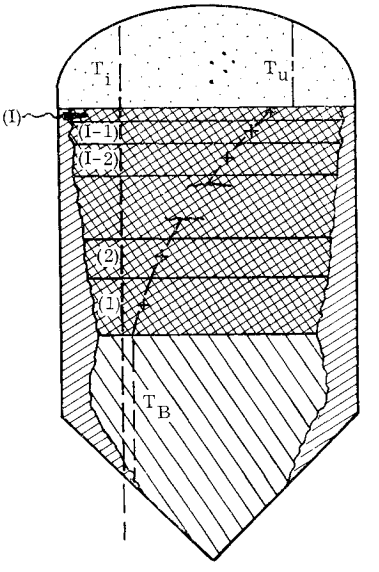

Fig. 5 The ith time step.

The layers are then repositioned in the vessel and the temperature gradients between layers and location of temperature gradient discontinuities are computed. The assumed temperature distribution is that obtained by connecting the mean temperature (assumed to be at layer centers) of adjacent layers (Fig. 5). The bottom of the first layer is at the unstratified temperature T_B, and the line connecting the top two layers is extended to the surface.

At the end of the ith time step i layers are formed (Fig. 5), each with a specified mass, average temperature, and position. In addition, all temperature gradients and discontinuities in temperature gradient (measured in the X coordinate) are specified, and the ullage has a specified mass, pressure, and average temperature. The program then proceeds to the next time step, and continues in a similar manner for a prescribed duration.

Boundary-Layer Equations

The three presently available analyses on turbulent natural convection boundary layers[9-11] differ considerably. The three analyses predict that the heat-transfer coefficient increases, is constant, and decreases, respectively, with boundary-layer run length. There is presently insufficient experimental data to definitely confirm any one. The analysis used here is based on Ref. 9 for constant wall temperature and revised to constant wall heat flux in Ref. 12. Reference 12 is outlined below for the specific case of interest here, namely, turbulent natural convection boundary layer in an axisymmetric vessel with constant heat flux and in the presence of a variable bulk temperature.

The differential-integral momentum and energy equations for this case are

$$\frac{d}{dx}\int_0^\delta (u^2R)dy = Rg\frac{dz}{dx}\int_0^\delta \left(\frac{\rho_L - \rho}{\rho_L}\right)dy - R\nu\left(\frac{du}{dy}\right)_w \quad (11)$$

$$\frac{d}{dx}\int_0^\delta (RuT)dy = T_L(x)\frac{d}{dx}\int_0^\delta (Ru)dy + \frac{Rq_w''}{\rho c_L} \quad (12)$$

The following assumptions apply: 1) the boundary layer is thin compared to the radius of the core, 2) the gravitational component normal to the wall is neglected, 3) the thermal and velocity boundary-layer thicknesses are equal, 4) except for density variation which affects the buoyant forces, properties are constant, 5) viscous heating is negligible, and 6) bulk temperature may vary but bulk velocity is zero.

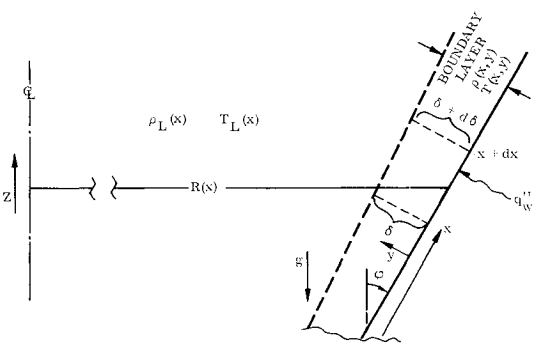

Fig. 6 Coordinate system.

The coordinate system used is shown in Fig. 6. From Ref. 9 the following relations are applied:

1) The turbulent natural convection boundary-layer velocity and temperature profiles ($u^* = 1.86\, u_{\max} = 6.83\bar{u}$):

$$u/u^* = (y/\delta)^{1/7}[1 - (y/\delta)]^4$$
$$(T - T_L)/(T_w - T_L) = [1 - (y/\delta)^{1/7}] \tag{13}$$

2) Wall shear stress:

$$\nu(du/dy)_w = 0.0225u^{*2}(\nu/\mu^*\delta)^{1/4} \tag{14}$$

3) The relation between heat flux and wall shear:

$$q_w'' = 0.0225\rho c_L u^*(T_w - T_L)(\nu/u^*\delta)^{1/4} \tag{15}$$

4) Linear coefficient of thermal expansion:

$$\beta = (\rho_L - \rho)/\rho_L(T - T_L) \tag{16}$$

Using the foregoing expressions in the momentum and energy equations, expressions for the thickness and velocity derivatives are:

$$\frac{d\delta}{dx} = -\frac{7}{9}\frac{\delta}{R}\frac{dR}{dx} - \frac{8}{9}E_1\frac{dT_L}{dx}\delta^{3/4}u^{*3/4} - \frac{M_1}{9}\frac{dz}{dx}\frac{\delta^{5/4}}{u^{*11/4}} + \left(\frac{8}{9}E_2 + \frac{1}{9}M_2\right)\frac{1}{u^{*1/4}\delta^{1/4}} \tag{17}$$

$$\frac{du^*}{dx} = -\frac{1}{9}\frac{u^*}{R}\frac{dR}{dx} + \frac{4}{9}E_1\frac{dT_L}{dx}\frac{u^{*7/4}}{\delta^{1/4}} + \frac{5}{9}M_1\frac{dz}{dx}\frac{\delta^{1/4}}{u^{*7/4}} - \left(\frac{4}{9}E_2 + \frac{5}{9}M_2\right)\frac{u^{*3/4}}{\delta^{5/4}} \tag{18}$$

where

$$M_1 = 106.2(\beta/\rho c_L)\nu^{-1/4}gq_w''$$
$$M_2 = 0.430\nu^{1/4}$$
$$E_1 = 0.090(\rho c_L/q_w'')\nu^{1/4} \tag{19}$$
$$E_2 = 0.614\nu^{1/4}$$

Equations (17) and (18), with $dR/dx = 0$ and $dz/dx = 1$, reduce to the momentum and energy equations for cylindrical geometry. Solutions for (17) and (18) of the power type can be obtained for either constant T_L or for T_L varying as $x^{-1/7}$, the latter being unrealistic and of little interest here. For the case of constant T_L, exact solutions to (17) and (18) for a pure cylinder are

$$\delta = (0.408)(\rho c_L\nu^3/\beta)^{1/14}(g^*q_w'')^{-1/14}x^{5/7}$$
$$u^* = (13.2)\nu(\beta/\rho c_L\nu^3)^{5/14}(g^*q_w'')^{5/14}x^{3/7} \tag{20}$$

For a pure cone (x measured from apex),

$$\delta = (0.241)(\rho c_L\nu^3/\beta)^{1/14}[g^*q_w''(dz/dx)]^{-1/14}x^{5/7}$$
$$u^* = (11.5)\nu(\beta/\rho c_L\nu^3)^{5/14}[g^*q_w''(dz/dx)]^{5/14}x^{3/7} \tag{21}$$

For an inclined flat plate,

$$\delta = (0.408)(\rho c_L\nu^3/\beta)^{1/14}[g^*q_w''(dz/dx)]^{-1/14}x^{5/7}$$
$$u^* = (13.2)\nu(\beta/\rho c_L\nu^3)^{5/14}[g^*q''_w(dz/dx)]^{5/14}x^{3/7} \tag{22}$$

Equations (20, 21, or 22) are used to obtain the initial values for boundary-layer integration depending on whether the boundary layer starts at the bottom of a cylinder, the apex of a cone, or in an inclined bottom, respectively. Equations (17) and (18) are then integrated numerically with distance along the vessel walls‡‡ at each computing time step to obtain δ and u^* as functions of x. The net mass and energy into or out of each layer is in turn computed for each time step using this δ and u^* data. From Eqs. (13) and (15), the mixed mean boundary-layer temperature T_{BL} is

$$T_{BL} = T_L + C_1q_w''\delta^{1/4}/\bar{u}^{3/4} \tag{23}$$
$$C_1 = 2.6/(\rho c_L\nu^{1/4})$$

It is found that on entering regions of very large bulk temperature gradient, Eqs. (17) and (18) predict δ and u^* to overshoot before approaching asymptotic values. In such cases, δ and u^* are evaluated from the relations

$$\delta = (0.633)(\nu/\beta^2\rho^3c_L^3)^{1/8}(q_w'')^{3/8}(g^*)^{-1/4}(dT_L/dx)^{-5/8} \tag{24}$$
$$u^* = (10.82)(\beta^2/\nu\rho^5c_L^5)^{1/8}(q_w'')^{5/8}(g^*)^{1/4}(dT_L/dx)^{-3/8}$$

which are approximate equations describing the asymptotic behavior of a turbulent natural convection boundary layer in a region of constant bulk temperature gradient. These equations were obtained by a fit of numerically evaluated asymptotic solutions to the boundary-layer equations. Using these values for δ and u^*, the integration proceeds normally.

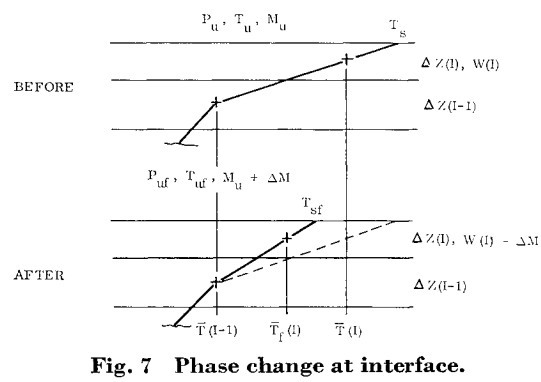

Fig. 7 Phase change at interface.

Interface Phase Change Routine

The model includes a routine[12] to permit interface energy and mass transfer, based on the simplifying assumption that equilibrium between the vapor and the liquid occurs when the ullage pressure and surface liquid vapor pressure are equal. Phase change is assumed to take place after the surface layer is deposited. If the surface liquid vapor pressure is greater than the ullage pressure as determined solely by the heat transfer $q_u\Delta\theta$ from the walls exposed to the ullage gas, vaporization will occur. If the ullage pressure is greater, condensation will occur. The "before" and "after" diagrams are shown in Fig. 7 (for the case of vaporization). It is assumed that 1) properties are constant, 2) the ullage gas behaves ideally, and 3) the phase change occurs at the mean surface temperature during the process. Three equations for the process are written 1) an energy balance on the sur-

‡‡ The boundary layer near the surface must turn 90° to spread out over the surface, and therefore, the two-dimensional boundary-layer equations are not valid in the immediate vicinity of the corner; however, in this model the boundary layer is assumed to approach the surface as though liquid were to continue above the surface.

face liquid layer, 2) an energy balance on the ullage gas, and 3) an equation of state relating surface liquid temperature and final ullage pressure. These equations are solved for the unknowns ΔM, $\bar{T}_f(i)$ and T_{uf}.

Discussion

Results for stratification of liquid hydrogen in a 40-in.-diam vessel with an elliptical bottom are presented in Figs. 8 and 9 at 120 and 300 sec, respectively. The wall heat flux, which is a result of radiation heat transfer through an evacuated jacket, is assumed to be spacially and time-wise uniform. Prior to the actual test, the vessel was vented to 14.2 psia to provide saturated liquid and vapor at the beginning of the test. Upon closing the vent valve the vessel is self-pressurized by a combination of heat transfer through the walls to the ullage gas and vaporization of stratified liquid at the surface.

The predictions of the temperature stratification for this case, using the stratified layer flow model are also shown on Figs. 8 and 9. In the prediction, the ullage heat rate used was 0.3 Btu/sec; the boundary layer was assumed to initiate at the junction of the cylinder and ellipse and the heat flux as obtained from pretest boiloff measurements was 67.2 Btu/ft²hr. The increase in tank pressure causes a significant increase in liquid hydrogen temperature due to the isentropic compression. This amounts to 0.07° and 0.14°R at the times 120 and 300 sec, respectively. In the comparison with the experimental data, the respective increments were added to the predicted temperature profiles, since the program does not account for the compressibility effect at this time. The predicted profiles are plotted in both a stepwise manner and in the manner of connecting the temperatures of adjacent layers with straight lines. It is seen that the program somewhat over-predicts the temperature near the surface and slightly under-predicts the temperature in the lower portion, but in general the agreement is quite good.

Tatom et al.[5] in analyzing the same data suggested that, since the temperature rise of the lower portion of the liquid was considerably greater than would be predicted by starting the boundary layer at the bottom of the cylinder, the bottom heating must seriously disrupt the boundary layer on the vertical walls causing significant energy transfer from the walls to the unstratified bulk liquid. However, the inclusion of the compressibility effect results in considerably better agreement between the experimental data and the prediction where the boundary layer starts at the bottom of the cylinder. Therefore, there appears to be only a slight effect of the bottom heating on disrupting the boundary layer on the vertical walls.

A series of schlieren photographs from Schwind and Vliet[7] of water stratification in a two-dimensional apparatus using electrical heating is shown in Fig. 10. The views show a 4-in.-square area (approximately) at the top corner of the vessel consisting of two 10-in.-high heated plates 6 in. apart. Figure 10a shows the initial surface flow (24 sec) and Figs. 10b and 10c at 90 and 140 sec, respectively, show the progression of stratification in the absence of the initial transients. Although the modified Rayleigh number for this case is approximately 10^{11} (near transition from laminar to turbulent flow), the photographs do point out some salient features of stratification which tend to confirm the model. It is seen that 1) the boundary layer on the vertical wall appears to be little affected by the vapor-liquid interface until very near the interface as is assumed in integrating the boundary-layer equations in the model; 2) the base of the stratified region appears to be quite horizontal (Fig. 10b), and although isotherms in the interior portion of the stratified region cannot be determined from the schlieren images it would seem that they are also nearly horizontal, which is in agreement with the one-dimensional temperature variation in the

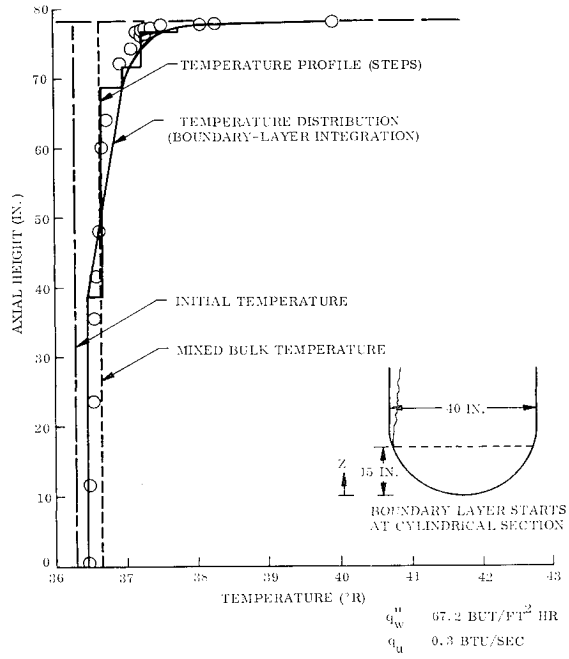

Fig. 8 Comparison of prediction with experimental data for liquid hydrogen stratification, 120 sec.

stratified region assumed in the model; and 3) the boundary layer appears to neck down as it enters and traverses the stratified region (Figs. 10b and 10c).

The theories for turbulent natural convection boundary layers of Eckert and Jackson,[9] Bayley[10] and Fujii[11] differ considerably. They predict that the heat-transfer coefficient increases, is constant, and decreases, respectively, with boundary-layer run length. The theory should be experimentally resolved as it is essential to the flow model. The assumption that the natural convection boundary layer on the inclined heated bottom of the vessel is unaffected by the normal buoyant force component is a reasonable assumption only for steep surfaces. For this reason, the boundary layer was assumed to start at the top of elliptical bottom in the

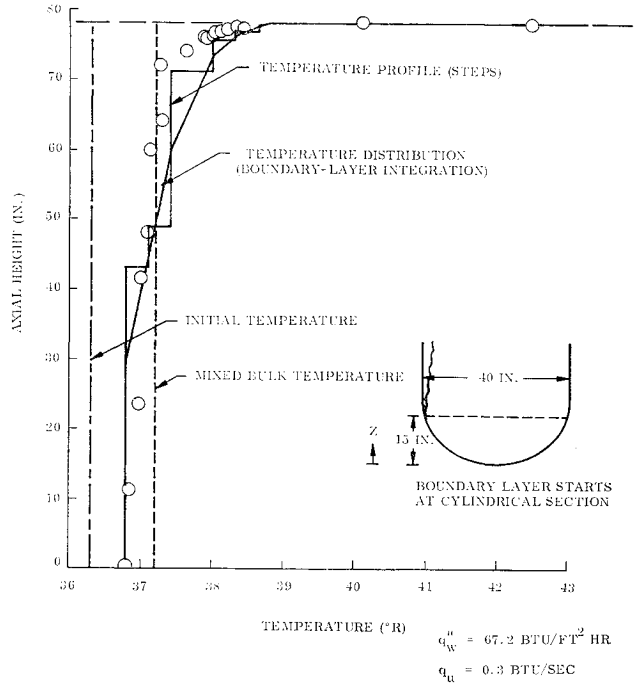

Fig. 9 Comparison of prediction with experimental data for liquid hydrogen stratification, 300 sec.

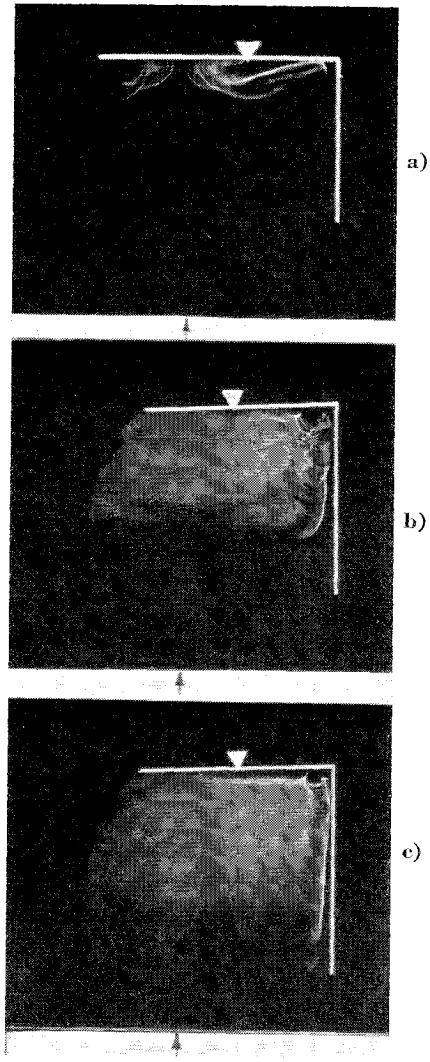

Fig. 10 Schlieren photographs of stratification.

preceding comparison since the major portion of the bottom is relatively flat. An adequate theory for natural convection flow on an inclined surface heated from below is also necessary.

Conclusions

The prediction of the stratified layer flow model appears to be in satisfactory agreement with experimental data, but further application of the model to other geometries, liquids, and heating and acceleration environments are advisable to prove its adequacy. A confirmation or improvement to the present turbulent natural convection boundary-layer theory on vertical surfaces and a theory for turbulent natural convection flow on inclined heated surfaces are required.

The model can be easily changed to predict stratification for laminar boundary layers by using presently available laminar natural convection boundary-layer theory. This model has also been extended to the case of a draining vessel with nuclear heating included and will be reported on in the future.

References

[1] Huntley, S. C., "Temperature-pressure-time relationships in a closed cryogenic container," Advan. Cryog. Eng. **3**, 342 (1957).

[2] Scott, L. E., Robbins, R. F., Mann, D. B., and Birmingham, B. W., "Temperature stratification in a non-venting liquid helium dewar," J. Res. Natl. Bur. Std. **64C**, 19 (1960).

[3] Bailey, T., Vande Koppel, R., Skartvedt, G., and Jefferson, T., "Cryogenic propellant stratification analysis and test data correlation," AIAA J. **1**, 1657 (1963).

[4] Bailey, T. and Fearn, R. F., "Analytical and experimental determination of liquid hydrogen temperature stratification," Advan. Cryog. Eng. **9**, 254 (1963).

[5] Tatom, J. W., Brown, W. H., Coxe, E. F., and Knight, L. H., "Analysis of thermal stratification of liquid hydrogen in rocket propellant tanks," Advan. Cryog. Eng. **9**, 265 (1963).

[6] Tellep, D. M. and Harper, E. Y., "Approximate analysis of propellant stratification," AIAA J. **1**, 1954 (1963).

[7] Schwind, R. G. and Vliet, G. C., "Observations and interpretations of natural convection and stratification in vessels," *Proceedings of the 1964 Heat Transfer and Fluid Mechanics Institute* (Stanford University Press, Stanford, Calif., 1964).

[8] Anderson, B. H. and Kolar, M. J., "Experimental investigation of the behavior of a confined fluid subjected to nonuniform source and wall heating," NASA TND-2079 (November 1963).

[9] Eckert, E. R. G. and Jackson, J. W., "Analysis of turbulent free-convection boundary layer on flat plate," NACA Rept. 1015 (1951).

[10] Bayley, F. J., "An analysis of turbulent free-convection heat transfer," Proc. Inst. Mech. Engs. **169**, 361 (1955).

[11] Fujii, T., "Experimental studies of free convection heat transfer," Jap. Soc. Mech. Engrs. **2**, 555 (1959).

[12] Vliet, G. C., "Stratified layer flow model-A numerical approach to temperature stratification in liquids contained in heated vessels," Lockheed Tech. Rept. 8-30-63-4 (November 1963).